IEEE Photonics Journal
An IEEE Photonics Society Publication

Open Access

Polarization Independent Unidirectional Scattering With Turnstile Nanoantennas

Volume 12, Number 6, December 2020

Davide Rocco
Michele Midrio
Costantino De Angelis

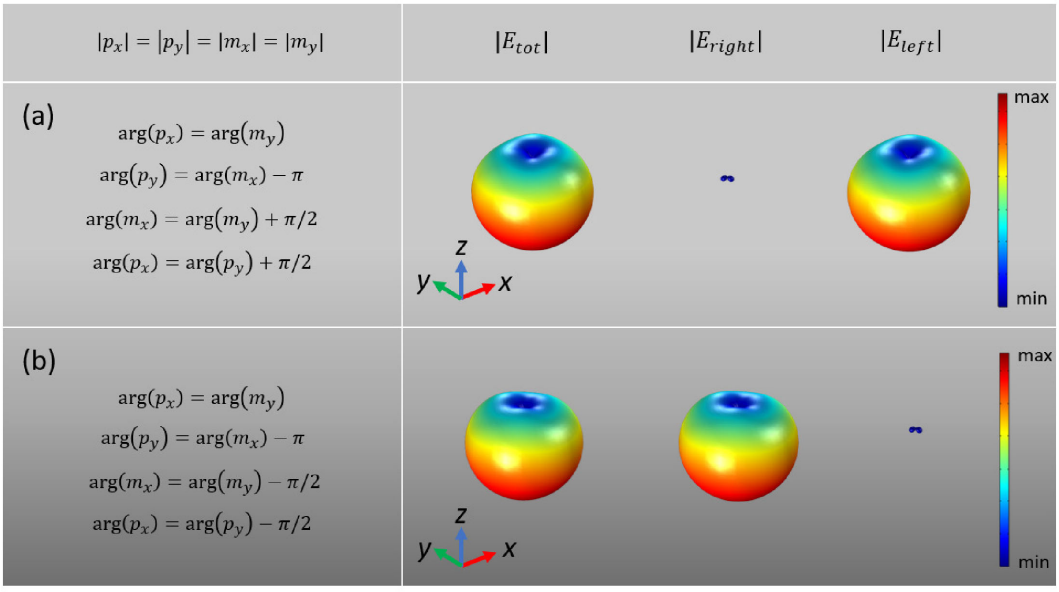

DOI: 10.1109/JPHOT.2020.3030306

Polarization Independent Unidirectional Scattering With Turnstile Nanoantennas

Davide Rocco [1,2] Michele Midrio,[3] and Costantino De Angelis [1,2]

[1]Department of Information Engineering, University of Brescia, via Branze 38, Brescia 25123, Italy
[2]National Institute of Optics, CNR-INO, via Branze 45, Brescia 25123, Italy
[3]CNIT, University of Udine, via delle Scienze 208, 33100 Udine, Italy

DOI:10.1109/JPHOT.2020.3030306

Manuscript received August 19, 2020; revised September 30, 2020; accepted October 8, 2020. Date of publication October 13, 2020; date of current version October 29, 2020. This work was supported by PRIN NOMEN. Corresponding author: Davide Rocco (e-mail: d.rocco003@unibs.it).

Abstract: We study the scattering behavior of a dielectric cross-dipole nanoantenna in the near-infrared spectral range when it is excited by a circular polarized plane wave. We theoretically demonstrate, for optimized geometrical parameters of the proposed turnstile structure, the possibility to simultaneously obtain a unidirectional scattering and a specific circular polarization of the scattered field. Our results open new functionalities for metamaterials and optical nanoantennas.

Index Terms: Optical resonator, metamaterials.

1. Introduction

Turnstile antennas have been extensively implemented in wireless communication systems at Radio Frequency (RF) mostly because they can generate isotropic, omnidirectional, dual-polarized, and circularly polarized (CP) radiation [1]–[3]. They are also commonly used for single-band, multi-band, and wideband operations [4]. In general, the turnstile antenna is made of two half-wavelength dipoles positioned at right angles with respect to each other in order to guarantee that the currents in the dipoles have the same amplitude and a phase quadrature difference [5]. Therefore, the turnstile antenna is also called a crossed dipole antenna. In its basic implementation, assuming that the dipoles lie in the *xy* plane, it has a near-isotropic radiation pattern in the Far-Field (FF) with a CP radiation in the out-of-plane directions (i.e., along the *z* axis). It has been shown that the front side of the FF emission radiates with one circular polarization, while the back side radiates with opposite circular polarization [6]. Since a large number of applications requires unidirectional radiation pattern, the RF crossed dipoles are often placed on a perfect electric conductor (PEC) reflector. The presence of the PEC surface reflects one-half of the emission into the opposite direction, thus achieving a unidirectional radiation pattern. Newly, different research group have demonstrated that the RF turnstile structure can be combined with different reflectors such as planar metallic, cavity-backed, and artificial magnetic conductor surfaces, to reach broad-band and one-side emission [7]–[9].

More recently, the turnstile antenna concept has been investigated at the nanoscale level where it has been firstly demonstrated optical cross antenna structure based on plasmonic resonances. In this scenario, the antenna consists of two perpendicular metallic nano-cuboids [10]–[11]–[12]. It has been demonstrated that the plasmonic cross antenna is able to convert propagating fields of any

polarization state into correspondingly polarized, localized, and enhanced fields and vice-versa. Additionally, it has been theoretically and experimentally investigated that the inhomogeneous space-time distribution of photogenerated hot carriers induces a transient symmetry breaking in a plasmonic metasurface made of highly symmetric gold nano-crosses resulting in a broadband transient dichroic optical response [13]. The main drawback of this new design is that plasmonic structures typically suffer of high absorption so the incident power must be carefully selected not to reach the melting point of the samples. However, dielectric materials can represent a reliable substitute at the nanoscale level [14]–[16]. Since the electric field can penetrate in this kind of structures, high-refractive-index nanoantennas induce electric and magnetic moments and support Mie modes in the visible and infrared spectral range. The use of dielectric nanoparticles not only permits to get access to magnetic optical response but also to drastically reduce the absorption losses associated with metals. All-dielectric nanoparticles, demonstrate a variety of unique effects such as the zero back-scattering of the emitted light in a pre-established direction without using PEC or reflector layers [17]–[20]. In fact, if electric and magnetic polarizabilities of a nanoparticle have the same amplitude and a specific phase shift, the light scattered from this nanostructure is null in the backward direction. This situation is commonly referred as Kerker condition [21]. More recently, several research studied and proposed extended and generalized Kerker conditions that are based on the interference of higher order multipole moments in the backward/forward direction in order to engineer the emission and the polarization of the scattered field at will [22]–[24]. In this scenario, silicon cross dipole nanoantenna have been studied to generate linearly polarized light with polarization angles ranging from 0° to 90° [25]. Moreover, planar all-dielectric chiral metasurface have been proposed for circular cross-polarization conversion [26]. Newly, the unidirectional scattered light controlled by incident polarized plane waves has gained a lot of attention in different context [27], [28]. In particular, the light intrinsic Quantum Spin Hall Effect feature has been deeply analyzed in [29]. The observation of such phenomena has been reported also in [30] where it has been proved that the transverse momentum and spin push and twist a Mie resonator in an evanescent field. Moreover, theoretically calculation of the interaction of two-wave field with probe Mie particles has been reported in [31] and experimentally verified in [32], [33]. Notably, in [34] it has been reported that the Mie theory can be used for the scattering of evanescent waves via rotation of its standard solutions by a complex angle. In all these situations, 2D or 3D structures that support surface modes with evanescent tails have counter-propagating modes with opposite transverse spins. This fundamental property of free-space Maxwell equations is independent of the nature of the interface, and is valid for any interfaces with evanescent waves. One of the most useful implementation of the transverse spin angular momentum is its ability to provide spin-controlled unidirectional propagation of light [35], [36]. Differently from the aforementioned works based on the transverse spin angular momentum, in this manuscript, we achieve the polarization independent unidirectional emission from a dielectric turnstile nanoantenna by optimizing the induced volume resonances inside the structure such as to achieve the desired behavior in the far-field emission.

By following the Mie theory formalism, we demonstrate the excitation of the Kerker condition in AlGaAs cross dipole nanoantenna in the near infrared regime when pumping light with left or right circular polarization. Moreover, we show, for the first time to our knowledge, that the unidirectional scattered field have a predominant (right or left) CP component depending on the incident field polarization, achieving a CP emission through a dielectric nanostructure with rotational symmetry. We thus propose our dielectric structure as a unidirectional scattering element with specific CP scattered field. We believe that these results may open new avenues for low-loss optical sources.

2. Results and Discussion

2.1 Theoretical Background

As a first example, let us consider the optical radiated far-field emitted by four dipoles: two orthogonal electric and two orthogonal magnetic ones. The four emitters are supposed to be place in close proximity one to each other with a distance in-between much more smaller than the

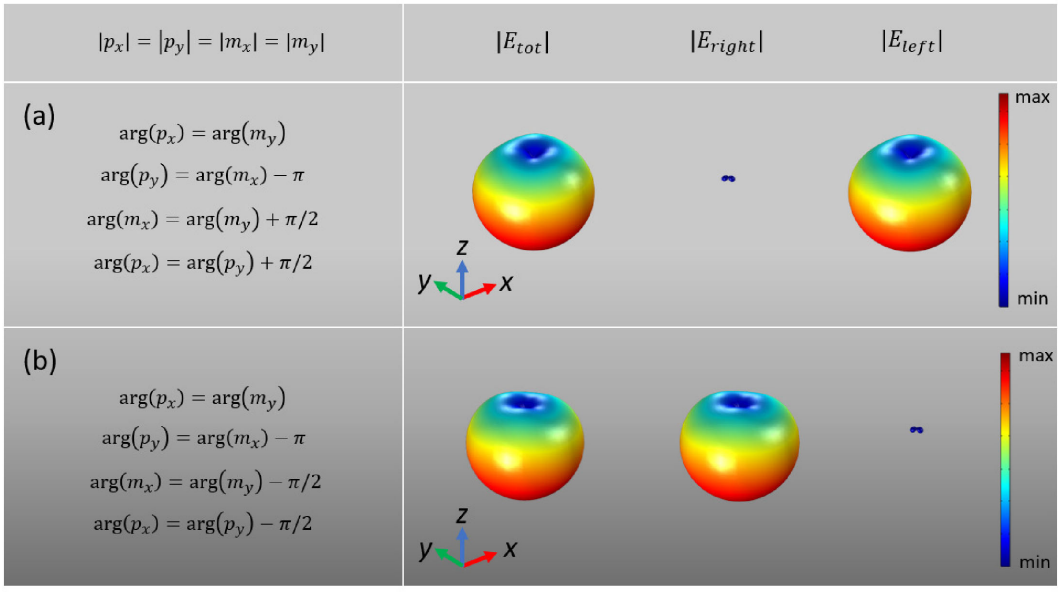

Fig. 1. The ideal case of four dipoles with same amplitude: p_x and p_y indicate the electric dipoles polarized along the *x* or *y* axis respectively while m_x and m_y represent the magnetic dipoles polarized along *x* or *y* direction. (a) The phase difference between the four emitters is chosen to achieve the first Kerker condition and to emit in the far-field mostly with left circular polarization while in (b) the phase shift is fixed to achieve the unidirectional emission and to obtain a radiation in the far-field mainly right circular polarized.

working wavelength. The dipoles are assumed to be placed in a homogenous medium assumed for simplicity to be air. For the purpose of our calculations we used a Cartesian basis. The electric dipolar contributions are named as p_α while the magnetic contributions are referred as m_α with $\alpha = x,y$ respectively. Two orthogonal electric dipoles can generate in the far field a near-isotropic radiation pattern with CP emission in the *z* direction [6]. In particular if $|p_x| = |p_y|$ and $arg(p_x) = arg(p_y)+\pi/2$ the scattered field is Right Circularly Polarized (RCP) along the $+z$ axis and Left Circularly Polarized (LCP) along the $-z$ direction. Indeed, if the phase difference between the electric dipoles is equal to -π/2 the emitted field has the opposite circular polarization with respect to the *z* direction. Similar considerations applies to the case of two radiating magnetic dipoles.

Here, we are assuming that the right component of the far field, E_{right}, is obtained as $E_{\mathrm{right}} = 1/\sqrt{2}(E_\theta + jE_\varphi)$ while the left one, E_{left}, is computed as $E_{\mathrm{left}} = 1/\sqrt{2}(E_\theta - jE_\varphi)$ knowing the spherical coordinate of the field. Moreover, it is known that the FF zero backscattered (first Kerker condition) is reached when $|p_x| = |m_y|$ and $arg(p_x) = arg(m_y)$ and equivalently when $|p_y| = |m_x|$ and $arg(p_y) = arg(m_x)-\pi$ [17]–[20]. Four electric and magnetic dipoles, (p_x, p_y, m_x, m_y) were designed to satisfy simultaneously all the previous conditions looking for a far-field characterized by a unidirectional emission that radiates with a specific CP component (right or left). In detail, Fig. 1(a) shows the scattered field in the case of fulfillment of the first Kerker condition and when a $+\pi/2$ rad phase difference between p_x and p_y and between m_x and m_y is selected. As one can observe, the FF is unidirectional with zero – backscattered signal and the radiation is almost completely LCP. Indeed, Fig. 1(b) represents a situation in which the first Kerker condition is still satisfied but the phase difference between p_x and p_y and between m_x and m_y is fixed to $-\pi/2$ rad. In this scenario, the total far-field amplitude remains unchanged but now the polarization is almost completely RCP due to the opposite phase difference between the electric and magnetic dipoles.

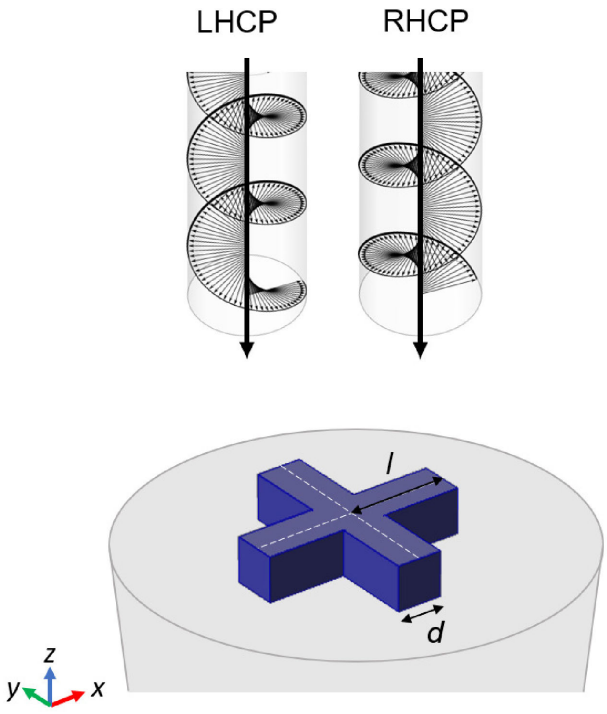

Fig. 2. Sketch of the proposed structure. The dielectric cross dipole antenna is assumed to be excited by a plane wave propagating in the $-z$ direction with a left or right circular polarization respectively.

2.2 Turnstile Nanoantenna Implementation

Thus, Fig. 1 represents the proof of concept of the idea of this work and guided us to implement a realistic design. The proposed solution is a dielectric cross dipole antenna made of AlGaAs. Recently, AlGaAs optical antennas have demonstrated higher effective control of the far-field scattering both in the linear and nonlinear regimes thanks to extremely low losses and the ability to sustain both electric and magnetic multipolar resonant optical modes [37]–[41]. The designed cross dipole is made of four cuboid with square side d and length l, as shown in Fig. 2. The dimension d is fixed to 200 nm and the far-field emission coming from the dielectric structure is studied by varying the length l between 500 and 900 nm. This initial parameters guess is done to guarantee the excitation of both electric and magnetic dipolar resonances in the structure. Attention is paid to limit as much as possible higher order multipoles which may translate into complicated radiation emission patterns [42]. For simplicity, and without loss of generality, the antenna is assumed to be placed in air. The turnstile antenna is illuminated by a normally incident circularly polarized plane wave of different handedness with pump wavelength in the range from 1500 nm to 1800 nm. We limit our analysis to the circular polarized light because the turnstile antenna is commonly associated with circular polarization behavior in the radio frequency range. However, due to the linear properties of the Maxwell equation our results hold also for linearly polarized light. We perform Finite Element Method numerical simulation in Comsol Multiphysics. The 3D mesh is customized to be more resolved in the cross-shape structure and at the interface between dielectric and air. The minimum mesh element size is less than 1 nm. To emulate the excitation of an isolated antenna, the domain is truncated by a Perfectly Matched Layer (PML), and the far-field emission is calculated on the inner boundary of the PML domain.

Fig. 3 shows the obtained results in terms of Far-Field Ratio (FFR) for the two incident polarization. The FFR is calculated as the ratio between the total far-field scattered along the $+z$ direction and the total far-field scattered along the $-z$ direction. This implies that the Kerker condition is

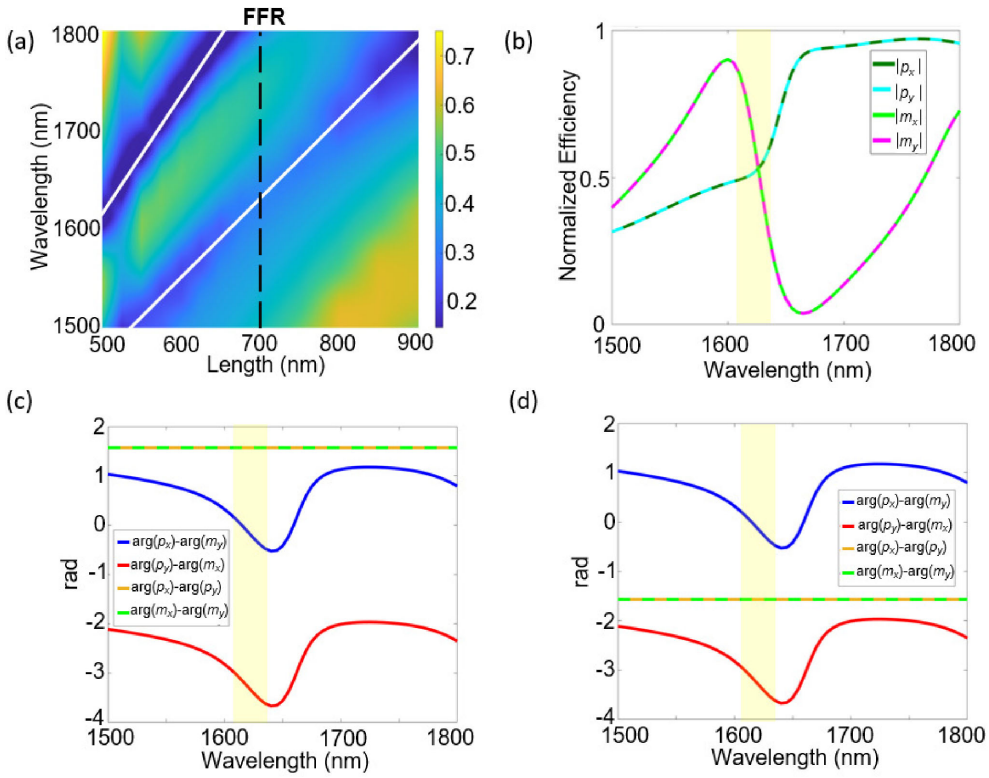

Fig. 3. (a) The FFR in the case of CP incident plane wave. (b) The normalized efficiency of the most excited dipolar contribution for a cross dipole nanoantenna with $l = 700$ nm and (c)-(d) their relative phase shift in the case of LHCP [RHCP] light excitation.

achieved when the FFR tends to zero. The white lines of Fig. 3(a) highlight the length l and corresponding incident wavelength at which the FFR is minimized. As an example, we consider the case of length equal to 700 nm as indicated by the black dotted lines in Fig. 3(a). For this geometry, the FFR has a minimum around 1630 nm. In order to gain a deeper insight of the obtained scattering behavior, a cartesian multipole decomposition, performed using the polarization currents induced inside the antenna, is carried out [43]. The obtained expansion indicates that the dominant contributions are the electric (p_x and p_y) and magnetic (m_x and m_y) dipolar ones. Notably, for an incident wavelength around 1630 nm, all the four contributions have the same amplitude, see Fig. 3(b). In particular at 1630 nm, it is possible to fulfill the first Kerker condition. We point out that the excited multipoles responses are strictly related to the entire cross-dipole antenna shape. Indeed, we verify that a single isolated cuboid does not achieve the unidirectional condition for the same wavelength of the turnstile structure. Moreover, as reported in the yellow region of Figs. 3(c) and (d), the phase difference between p_x and m_y is almost equal to zero and the phase difference between p_y and m_x is almost equal to $-\pi$ rad and this confirms that the minimum in the FFR is due to the attainment of the first Kerker condition. It is also important to notice that the phase difference between p_x, p_y and between m_x, m_y is equal to $+\pi/2$ rad for LCP incident light and to $-\pi/2$ rad for RCP, as imposed by the symmetry of the cross-dipole structure.

The quadrature phase shift between the two electric and the two magnetic dipole implies that the scattered field has a predominant left or right CP component when the pump beam is LCP or RCP, respectively. We estimate 4 orders of magnitude difference in the two CP component along the $-z$ axis direction. Fig. 4(a) show the normalized CP (left or right) component in the scattered field ($-z$ direction) together with the wavelength at which the first Kerker condition is achieved as

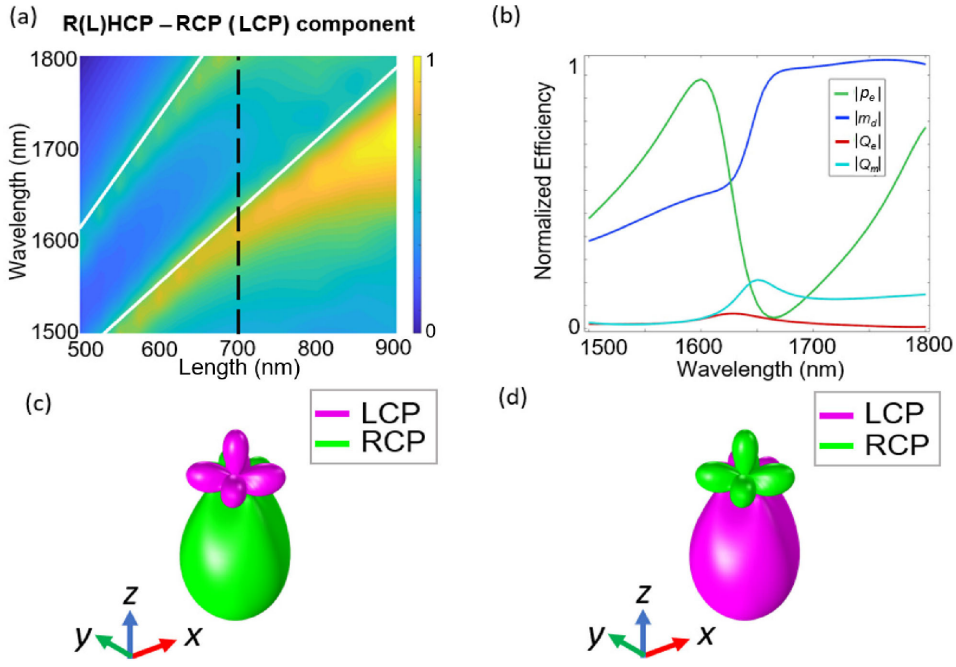

Fig. 4. (a) The RCP (LCP) Far-Field along the $-z$ direction for the case of RHCP (LHCP) incident plane wave. The CP component is normalized to its maximum. (b) The Cartesian multipolar decomposition. (c) The total Far-Field for the case of RHCP incident plane wave and (d) The total far-field for LHCP excitation decomposed in the LCP (magenta) and RCP (green) component.

indicated by the white lines. It is possible to observe that there are regions for which the maximum in the right/left polarization component is achieved when the unidirectional emission is obtained. In particular, for a length *l* equal to 700 nm it is possible to reach the unidirectional emission around 1630 nm but also the scattered field has a maximum left/right polarization contribution depending on the incident CP field. Moreover, Figs. 4(c) and (d) show the total far-field scattered by the selected turnstile antenna at 1630 nm decomposed in its right and left circular polarization contribution for the two different incident polarizations. It is possible to notice that, for a particular choice of the geometrical parameters, the dielectric nanoantenna is able to scatter light mostly in the forward direction and with a predominant RCP or LCP contribution in the far-field. Thus, the proposed structure is capable to act as a unidirectional emitter with specific circular polarization emission properties. Please note that, although the scattering behavior is dominated by the electric and magnetic dipolar contribution, there are also small quadrupolar contribution (either electric Q_e and magnetic Q_m) that affect the radiation as can be noticed in Fig. 4(b) and in the obtained FF emission, see Figs. 4(c) and (d). Moreover, we point out that, for the proposed cross dipole nanoantenna, the transmission circular dichroism (CD) is zero because the structure presents an in-plane mirror symmetry. In fact, the CD is defined as the difference in the total transmission for LCP incident light with respect to the total transmission for RCP pump. For the studied design, the total transmissions have the same absolute value for both excitation fields (i.e., CD $= 0$) but present opposite circular polarization in the far-field. The interested reader may also refers to Refs. [44]–[46].

3. Conclusion

In this work, we have demonstrated the possibility to use a dielectric cross dipole antenna to simultaneously fulfill the so called Kerker condition and to engineer a desired CP radiation of the

unidirectional radiated light. We believe that this result may open new scenarios for designing compact and circular polarization selective optical sources, with an important step toward the development of tunable metasurfaces.

Acknowledgment

The authors wish to thank the anonymous reviewers for their valuable suggestions.

References

[1] T. S. Xuat, I. Park, and R. W. Ziolkowski, "Crossed dipole antennas: A review," *IEEE Antennas Propag. Mag.*, vol. 57, no. 5, pp. 107–122, Oct. 2015.
[2] I. Radnović, A. Nešić, and B. Milovanović, "A new type of turnstile antenna," *IEEE Antennas Propag. Mag.*, vol. 52, no. 5, pp. 168–171, Oct. 2010.
[3] P. Guoping, Y. Li, Z. Zhang, and Z. Feng, "Isotropic radiation from a compact planar antenna using two crossed dipoles," *IEEE Antennas Wireless Propag. Lett.*, vol. 11, pp. 1338–1341, Nov. 2012.
[4] C. Deng, Y. Li, Z. Zhang, and Z. Feng, "A wideband isotropic radiation planar antenna using sequential rotated L-shaped monopoles," *IEEE Trans. Antennas Propag.*, vol. 62, no. 3, pp. 1461–1464, Mar. 2014.
[5] G. H. Brown, "The turnstile antenna," *Electron.*, vol. 9, no. 15, pp. 14–17, Apr. 1936.
[6] S. GM Darwish, K. FA Hussein, and H. A. Mansour, "Circularly polarized crossed-dipole turnstile antenna for satellites," in *Proc. Twenty-1st Nat. Radio Sci. Conf.*, 2004, Art. no. B17-1.
[7] JM. Baracco, L. Salghetti-Drioli, and P. de Maagt, "AMC low profile wideband reference antenna for GPS and GALILEO systems," *IEEE Trans. Antennas Propag.*, vol. 56, no. 8, pp. 2540–2547, Aug. 2008.
[8] R. Wakabayashi, K. Shimada, H. Kawakami, and G. Sato, "Circularly polarized log-periodic dipole antenna for EMI measurements," *IEEE Trans. Electromagn. C*, vol. 41, no. 2, pp. 93–99, May 1999.
[9] G. Liu, L. Xu, and Z. Wu, "Miniaturised wideband circularly-polarised log-periodic koch fractal antenna," *Electron. Lett.*, vol. 49, no. 21, pp. 1315–1316, Oct. 2013.
[10] P. Biagioni, M. Savoini, J. S. Huang, L. Duò, M. Finazzi, and B. Hecht, "Near-field polarization shaping by a near-resonant plasmonic cross antenna," *Phys. Rev. B*, vol. 80, no. 15. Oct. 2019, Art. no. 153409.
[11] P. Biagioni, J. S. Huang, L. Duò, M. Finazzi, and B. Hecht, "Cross resonant optical antenna," *Phys. Rev. Lett.*, vol. 102, no. 25, Jun. 2009, Art. no. 256801.
[12] C. De Angelis, A. Locatelli, D. Modotto, S. Boscolo, M. Midrio, and A. D. Capobianco, "Frequency addressing of nano-objects by electrical tuning of optical antennas," *J. Opt. Soc. Am. B*, vol. 27, no. 5, pp. 997–1001, May 2010.
[13] A. Schirato *et al.*, "Transient optical symmetry breaking for ultrafast broadband dichroism in plasmonic metasurfaces," *arXiv:2008.00079*..
[14] M. Caldarola *et al.*, "Non-plasmonic nanoantennas for surface enhanced spectroscopies with ultra-low heat conversion," *Nat. Commun.*, vol. 6, no. 1, pp. 1–8, Aug. 2015.
[15] P. Albella *et al.*, "Low-loss electric and magnetic field-enhanced spectroscopy with subwavelength silicon dimers," *J. Phys. Chem. C*, vol. 117, no. 26, pp. 13573–13584, May 2013.
[16] A. E. Krasnok, A. E. Miroshnichenko, P. A. Belov, and Y. S. Kivshar, "All-dielectric optical nanoantennas," *Opt. Express*, vol. 20, no. 18, pp. 20599–20604, Aug. 2012.
[17] B. Rolly, B. Stout, and N. Bonod, "Boosting the directivity of optical antennas with magnetic and electric dipolar resonant particles," *Opt. Express*, vol. 20, no. 18, pp. 20376–20386, Aug. 2012.
[18] D. Rocco, L. Carletti, A. Locatelli, and C. De Angelis, "Controlling the directivity of all-dielectric nanoantennas excited by integrated quantum emitters," *J. Opt. Soc. Am. B*, vol. 34, no. 9, pp. 1918–1922, Aug. 2017.
[19] A. E. Krasnok, C. R. Simovski, P. A. Belov, and Y. S. Kivshar, "Superdirective dielectric nanoantennas," *Nanoscale*, vol. 6, no. 13, pp. 7354–7361, Apr. 2014.
[20] W. Zhao *et al.*, "Dielectric huygens' metasurface for high-efficiency hologram operating in transmission mode," *Sci. Rep.*, vol. 6, Jul. 2016, Art. no. 30613.
[21] M. Kerker, D. S. Wang, and C. L. Giles, "Electromagnetic scattering by magnetic spheres," *J. Opt. Soc. Am.*, vol. 73, no. 6, pp. 765–767, Jun. 1983.
[22] R. Alaee, R. Filter, D. Lehr, F. Lederer, and C. Rockstuhnl, "A generalized kerker condition for highly directive nanoantennas," *Opt. Lett.*, vol. 40, no. 11, pp. 2645–2648, Jun. 2015.
[23] A. Pors, S. K. H. Andersen, and S. I. Bozhevolnyi, "Unidirectional scattering by nanoparticles near substrates: Generalized kerker conditions," *Opt. Express*, vol. 23, no. 22, pp. 28808–28828, Nov. 2015.
[24] J. van de Groep and A. Polman, "Designing dielectric resonators on substrates: Combining magnetic and electric resonances," *Opt. Express*, vol. 21, no. 22, pp. 26285–26302, Nov. 2013.
[25] X. Cai, Z. Li, Y. Kong, D. Lu, Y. Wei, and L. Huang, "Tunable polarization rotation using non-chiral all-dielectric metasurfaces," *Optik*, vol. 207, Nov. 2019, Art. no. 163769.
[26] Z. Ma, Y. Li, Y. Li, Y. Gong, S. A. Maier, and M. Hong, "All-dielectric planar chiral metasurface with gradient geometric phase," *Opt. Express*, vol. 26, no. 5, pp. 6067–6078, Mar. 2018.
[27] K. Y. Bliokh and F. Nori, "Transverse and longitudinal angular momenta of light," *Phys. Rep.*, vol. 592, pp. 1–38, Aug. 2015.
[28] K. Y. Bliokh, F. J. Rodriguez-Fortuno, F. Nori, and A. V. Zayats, "Spin-orbit interactions of light," *Nat. Photon.*, vol. 9, no. 12, pp. 796–808, Nov. 2015.

[29] K. Y. Bliokh, D. Smirnova, and F. Nori, "Quantum spin hall effect of light," *Science*, vol. 348, no. 6242, pp. 1448–1451, Jun. 2015.
[30] K. Y. Bliokh, A. Y. Bekshaev, and F. Nori, "Extraordinary momentum and spin in evanescent waves," *Nat. Commun.*, vol. 5, no. 1, pp. 1–8, Mar. 2014.
[31] A. Y. Bekshaev, K. Y. Bliokh, and F. Nori, "Transverse spin and momentum in two-wave interference," *Phys. Rev. X*, vol. 5, no. 1, Mar. 2015, Art. no. 011039.
[32] M. Antognozzi *et al.*, "Direct measurements of the extraordinary optical momentum and transverse spin-dependent force using a nano-cantilever," *Nat. Phys.*, vol. 12, no. 8, pp. 731–735, Apr. 2016.
[33] L. Liu, A. D. Donato, V. Ginis, S. Kheifets, A. Amirzhan, and F. Capasso, "Three-Dimensional measurement of the helicity-dependent forces on a mie particle," *Phys. Rev. Lett.*, vol. 120, no. 22, May 2018, Art. no. 223901.
[34] A. Y. Bekshaev, K. Y. Bliokh, and F. Nori, "Mie scattering and optical forces from evanescent fields: A complex-angel approach," *Opt. Express*, vol. 21, no. 6, pp. 7082–7095, Mar. 2013.
[35] Y. Lefier and G. Thierry, "Unidirectional sub-diffraction waveguide based on optical spin-orbit coupling in subwavelength plasmonic waveguide," *Opt. Lett.*, vol. 40, no. 12, pp. 2890–2893, Jun. 2015.
[36] F. J. Rodriguez-Fortuno *et al.*, "Near-field interference for the unidirectional excitation of electromagnetic guided modes," *Science*, vol. 340, no. 6130, pp. 328–330, Apr. 2013.
[37] D. Rocco *et al.*, "Vertical second harmonic generation in asymmetric dielectric nanoantennas," *IEEE Photon. J*, vol. 12, no. 3, Jun. 2020, Art. no. 4500507.
[38] L. Ghirardini *et al.*, "Shaping the nonlinear emission pattern of a dielectric nanoantenna by integrated holographic gratings," *Nano Lett.*, vol. 18, no. 11, pp. 6750–6755, Oct. 2018.
[39] D. Rocco *et al.*, "Switching the second harmonic generation by a dielectric metasurface via tunable liquid crystal," *Opt. Express*, vol. 28, no. 8, pp. 12037–12046, Apr. 2020.
[40] G. Marino *et al.*, "Zero-order second harmonic generation from algaas-on-insulator metasurfaces," *ACS Photon.*, vol. 6, no. 5, pp. 1226–1231, Apr. 2019.
[41] D. Rocco, M. A. Vincenti, and C. De Angelis, "Boosting second harmonic radiation from algaas nanoantennas with epsilon-near-zero materials," *Appl. Sci.*, vol. 8, no. 11, Nov. 2018, Art. no. 2212.
[42] V. F. Gili *et al.*, "Monolithic algaas second-harmonic nanoantennas," *Opt. Express*, vol. 24, no. 14, pp. 15965–15971, Jul. 2016.
[43] E. E. Radescu and G. Vaman, "Exact calculation of the angular momentum loss, recoil force, and radiation intensity for an arbitrary source in terms of electric, magnetic, and toroid multipoles," *Phys. Rev. E*, vol. 65, no. 4, Apr. 2002, Art. no. 046609.
[44] F. R. Gómez, J. R. Mejía-Salazar, and P. Albella, "All-dielectric chiral metasurfaces based on crossed-bowtie nanoantennas," *ACS Omega*, vol. 4, no. 25, pp. 21041–21047, Dec. 2019.
[45] K. Y. Bliokh, A. Y. Bekshaev, and F. Nori, "Optical momentum, spin and angular momentum in dispersive media," *Phys. Rev. Lett.*, vol. 119, no. 7, Aug. 2017, Art. no. 073901.
[46] M. F. Picardi, K. Y. Bliokh, F. J. Rodríguez-Fortuno, F. Alpeggiani, and F. Nori, "Angular momenta, helicity, and other properties of dielectric-fiber and metallic-wire modes," *Optica*, vol. 5, no. 8, pp. 1016–1026, Aug. 2018.